LBL-36747
UC-413
Preprint

Lawrence Berkeley Laboratory

UNIVERSITY OF CALIFORNIA

Submitted to Physical Review C

Dilepton Production from Pion Annihilation in a Realistic Delta-Hole Model

J. Helgesson and J. Randrup

April 1995

Prepared for the U.S. Department of Energy under Contract Number DE-AC03-76SF00098

DISCLAIMER

Physical Review C LBL-36747

Dilepton production from pion annihilation in a realistic delta-hole model *

Johan Helgesson and Jørgen Randrup

Nuclear Science Division, Lawrence Berkeley Laboratory
University of California, Berkeley, California 94720

April 14, 1995

*This work was supported by the Swedish Natural Science Research Council, the National Institute for Nuclear Theory at the University of Washington in Seattle, and by the Director, Office of Energy Research, Office of High Energy and Nuclear Physics, Nuclear Physics Division of the U.S. Department of Energy under Contract No. DE-AC03-76SF00098.

Dilepton production from pion annihilation in a realistic delta-hole model

Johan Helgesson and Jørgen Randrup
Nuclear Science Division, Lawrence Berkeley Laboratory, University of California, Berkeley, California 94720
(April 14, 1995)

Dilepton production from $\pi^+\pi^-$ annihilation in nuclear matter is calculated in a simple two-level delta-hole model and a more realistic model including both real pions and nucleon-hole and delta-hole excitations. Substantial enhancement of the dilepton yield is found in the invariant mass region $M < 250$ MeV/c^2 due to annihilation of non-collective low-energy high-momentum nucleon-hole modes having a (very) small pion component. The inclusion of a finite temperature in the dispersion relation does not affect the total dilepton yield much, although it causes significant redistribution of the contributions from the various combinations of pionic modes.

PACS numbers: 25.70.-z, 25.75.+r

Dilepton production is a promising tool for studying the hot and dense nuclear medium, since final-state interactions are very weak, as first pointed out by Gale and Kapusta [1,2]. In a schematic model of nuclear matter, they considered dileptons arising from different processes, using relativistic kinetic theory. The production of dileptons from $\pi^+\pi^-$ annihilation was found to depend sensitively on the dispersion relation of the pionic mode. The treatment was later improved in ref. [3] by deriving the dispersion relations of the pionic modes in a simple two-level ΔN^{-1} model consisting of a pion and a ΔN^{-1} state. Additional improvements were subsequently made, such as investigating the effect of the imaginary part of the pion self energy [4] and including vertex corrections to the electromagnetic interaction [5,6].

Part of these results have, with a varying degree of sophistication, been used in both fireball [3] and transport [7–10] models to describe dilepton production in heavy-ion collisions. However, a simple two-level ΔN^{-1} model has been used throughout to obtain the dispersion relation of the pionic modes. In this note we reconsider dilepton production from $\pi^+\pi^-$ annihilation in nuclear matter, employing a more realistic model that includes both NN^{-1} and ΔN^{-1} excitations as well as pions.

Transport simulations of heavy-ion collisions predict the production of dileptons from a variety of processes [7–10]. At low invariant mass ($M\approx$200–400 MeV) the dominant channels are η and Δ Dalitz decay and pn bremsstrahlung [10]. The contribution from $\pi^+\pi^-$ annihilation starts to be important only at invariant masses around $M \approx 500$ MeV, but it becomes the dominant process for larger invariant masses. Since the $\pi^+\pi^-$ contribution to the dilepton yield at $M\approx$600–900 MeV is mainly determined by the pion electromagnetic form factor, it may then be difficult to extract information about the in-medium pion properties from dilepton production in heavy-ion collisions. However, the dilepton production processes used in the semi-classical transport simulations have been based mainly on vacuum properties and so the predictions are correspondingly uncertain. Moreover, the previous investigations of dilepton production from $\pi^+\pi^-$ annihilation used either the free pion dispersion relation or the simple two-level ΔN^{-1} model, which neglects the continuum of NN^{-1} states and compresses the continuum of ΔN^{-1} states to a single state.

The pionic (or spin-isospin) modes can be calculated within the RPA approximation including π, NN^{-1}, and ΔN^{-1} degrees of freedom. The resulting modes generally contain components of all these states and, consequently, when two such modes annihilate into a dilepton pair there are different processes involved, depending on which component in the spin-isospin mode is realized ($\pi+\pi$, $\pi+NN^{-1}$, $\pi+\Delta N^{-1}$, etc.), and the appropriate electromagnetic vertex should be used, together with the squared amplitude of the corresponding component of the spin-isospin mode. The first investigations of dilepton production from annihilation of pionic modes considered only the $\pi+\pi$ contributions [3,4]. Subsequent studies including also the $\pi+\Delta N^{-1}$ contributions [5,6] found that these vertex corrections reduce the dilepton yield. But the effect is rather small when the Δ width is included self-consistently [6]. Since the $\pi+\pi$ components give the dominant contribution to the dilepton production from annihilation of spin-isospin modes, we will concentrate on comparing the contribution to the dilepton production from the $\pi+\pi$ components using the simple two-level ΔN^{-1} model and a more realistic $\pi+NN^{-1}+\Delta N^{-1}$ model [11].

Following ref. [11], we calculate the dispersion relation in a non-relativistic RPA formalism, treating interactions between pions, nucleon-hole, and Δ-hole states. The interactions contain a standard p-wave interaction and a short-range g'-type interaction. This yields the energies of all the eigenmodes and their expansion amplitudes on the various elementary excitations.

The dispersion relation is shown in fig. 1 for normal nuclear density, $\rho=\rho_0$, and at zero temperature, T=0. Our choice of parameter values was discussed in detail in ref. [11] and is summarized in table I. There are two collec-

$m_N = 940$ MeV/c^2	$g'_{NN} = 0.9$	$f^\pi_{NN} = 1.0$
$m_\Delta = 1230$ MeV/c^2	$g'_{N\Delta} = 0.38$	$f^\pi_{N\Delta} = 2.2$
$m_\pi = 140$ MeV/c^2	$g'_{\Delta\Delta} = 0.35$	$f^\pi_{\Delta\Delta} = 0$
$m_\rho = 770$ MeV/c^2	$\Lambda_g = 1.5$ GeV	$\Lambda^\pi = 1.0$ GeV
$\rho_0 = 0.153$ fm^{-3}	$m^*_N = m_N/[1+0.4049(\rho/\rho_0)]$	

TABLE I. Parameter values employed in the calculations.

tive modes, corresponding to those of the simple two-level model. They are often referred to as the pion and ΔN^{-1} branch, respectively. Since they are both pion-like we will refer to them as $\tilde{\pi}_1$ (lower) and $\tilde{\pi}_2$ (upper) [11].

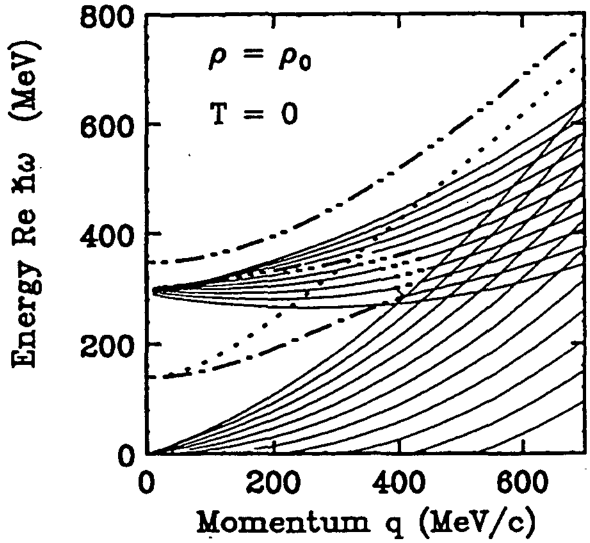

FIG. 1. The spin-longitudinal spin-isospin modes in nuclear matter at normal density and zero temperature, as obtained with the $\pi + NN^{-1} + \Delta N^{-1}$ model. The non-collective modes are shown by solid curves, while collective modes are represented by either a dot-dashed curve ($\tilde{\pi}_1$), a dot-dot-dashed curve ($\tilde{\pi}_2$), or a dot-dot-dot-dashed curve (for other modes with some collective strength). The free pion dispersion relation is shown as the dotted curve.

In addition we obtain a number of NN^{-1} or ΔN^{-1} like modes. These modes are mainly non-collective, each being dominated by a single NN^{-1} or ΔN^{-1} component. The appearance of non-collective modes in the formalism requires special attention. Although non-collective in character, these modes will aquire a small pion component in the wave function (usually <1%). The annihilation of the pionic component in a non-collective mode will thus contribute to the dilepton yield.

The collective modes are well described by Bose-Einstein statistics, since their strength is spread over a large number of elementary excitations, so the mean number of collective modes n_j is given by $n_j(\omega,T) \approx [\exp(\omega/T)-1]^{-1}$. By contrast, the non-collective modes are dominated by a single baryon-hole exciton which is thereby exhausted. Therefore, the mean number of non-collective modes in the state j is given by $n_j(\omega,T) \approx [\exp(\omega/T)+1]^{-1}$. This is an important feature, because those non-collective NN^{-1} modes that have very small $\omega_j(q)$ for finite momenta q would be drastically overpopulated if Bose-Einstein statistics were used (even to the extent of diverging in the limit $\omega_j \to 0$).

In infinite nuclear matter at temperature T and density ρ we calculate the dilepton production rate from $\pi^+\pi^-$ annihilation according to [1,3],

$$\left.\frac{d^8N^{e^+e^-}_{\pi\pi}}{d^4xd^3qdM}\right|_{q=0} = \frac{\alpha^2|F_\pi(M)|^2}{6\pi^4M^2}\sum_{j,j'}\int_0^M d\omega \int dq \frac{q^4}{\omega_\pi(q)^2} \times n_j(\omega)n_{j'}(M-\omega)S^j_\pi(\omega,q)\, S^{j'}_\pi(M-\omega,q)\,, \quad (1)$$

where we take

$$S^j_\pi(\omega,q) = -\frac{1}{\pi}\, P^j_\pi(\omega,q)\ \mathrm{Im}\,\frac{1}{\omega-\omega_j(q)+i\delta}\,, \quad (2)$$

with $P^j_\pi(\omega,q)$ being the squared amplitude of the pion component along the mode j. Note that $S^j_\pi(\omega,q)$ is related to the pion spectral function $S_\pi(\omega,q)$ and the pion propagator $D_\pi(\omega,q)$, by

$$S_\pi(\omega,q) = -\frac{1}{\pi}\ \mathrm{Im}\ D_\pi(\omega,q) = -\frac{1}{2\omega}\sum_j S^j_\pi(\omega,q)\,. \quad (3)$$

The factor $1/\omega_\pi(q) = [m_\pi^2+q^2]^{-\frac{1}{2}}$ originates from the normalization of the elementary pion fields.

In fig. 2 we present the calculated total dilepton production rate at different nuclear densities, for T=100 MeV. In fig. 2a we have used the dispersion relations from the simple two-level model used in previous works, while in 2b the more realistic $\pi + NN^{-1} + \Delta N^{-1}$ model of ref. [11] has been used. In both calculations, Γ_Δ and T were taken to be zero in the dispersion relations, although, for numerical reasons, a small but finite value was employed for the imaginary part δ in eqs. (2) and (3). This also removes any singularities in the dilepton yield arising from a possible minimum in the dispersion relation. Such singularities are also regularized when the Δ width is included self-consistently in the dispersion relations [4] and we have found that the results in fig. 2 are rather unaffected by this refinement.

We see that while the dilepton production rate approaches zero at invariant masses smaller than approximately 250 MeV in fig. 2a, there is a substantial contribution in fig. 2b. The latter originates from annihilation of one or two of the non-collective NN^{-1} states. Even though the pion component of these modes is very small, about 0.2% at normal density, they give a large contribution since they contribute at high momenta q and the dilepton yield in eq. (1) is enhanced by the factor q^4. The effect increases with density because the pion component in the NN^{-1} states is enhanced. This effect is naturally absent in fig. 2a where the NN^{-1} states not are included. As the nuclear density is increased the pionic mode $\tilde{\pi}_1$ is softened. This causes the mode to enter the NN^{-1} continuum (before the ΔN^{-1} continuum) at a lower energy and smaller momentum than at lower densities. The non-collective NN^{-1} modes will then have larger pionic admixtures. As the density is increased further, the system approaches pion condensation and low-energy acoustic modes with a relatively large pion component appear. Annihilation of such low-energy modes give a large contribution to the dilepton yield at low invariant mass, as seen in fig. 2b. With our choice of parameters, the onset of pion condensation appears around $\rho \approx 2\rho_0$, and is fully developed at $\rho \approx 3\rho_0$. The effect can be pushed up in density by increasing the values of $g'_{N\Delta}$ and $g'_{\Delta\Delta}$, for example by making them density dependent.

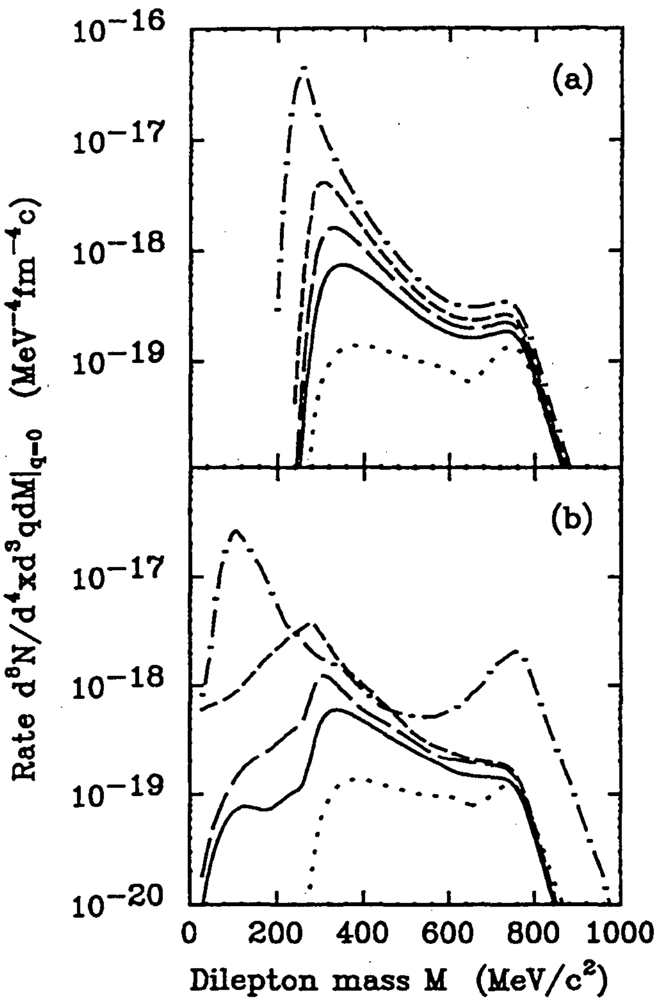

FIG. 2. Total dilepton production rate at calculated at T=100 MeV with the simple two-level ΔN^{-1} model (a) and the more realistic $\pi + \Delta N^{-1} + NN^{-1}$ model (b) at the densities ρ=0 (dotted), $\rho=\rho_0$ (solid), $\rho=1.5\rho_0$ (long-dashed), $\rho=2\rho_0$ (short-dashed), and $\rho=3\rho_0$ (dot-dashed). (The dispersion relations have been calculated using T=0.)

We have also investigated the effect of calculating the dispersion relations at T=100 MeV. Although our model [11] contains the assumption that the Fermi and Bose occupation factors n_Δ and n_π are small, we can still obtain a first estimate of the temperature effect on the dilepton production rate. Relative to T=0, there are naturally many more NN^{-1} and ΔN^{-1} modes. Moreover, the collective modes $\tilde{\pi}_1$ and $\tilde{\pi}_2$ are changed somewhat: the upper collective mode $\tilde{\pi}_2$ is lowered in energy, while the mode $\tilde{\pi}_1$ loses its collective strength somewhat earlier (smaller q). The total dilepton rate is not affected much, but the contribution from specific combinations of basic modes is redistributed relative to T=0.

Figure 3 shows the dilepton rate at normal density together with the contributions from specific combinations of annihilated modes. The dispersion relations have been calculated using T=100 MeV. In the two-level model (fig. 3a) there are only the two modes $\tilde{\pi}_1$ and $\tilde{\pi}_2$, so there are only three possible combinations: $\tilde{\pi}_1 + \tilde{\pi}_1$, $\tilde{\pi}_1 + \tilde{\pi}_2$, and $\tilde{\pi}_2 + \tilde{\pi}_2$. Of these, $\tilde{\pi}_1 + \tilde{\pi}_1$ is the dominant one (long-dashed curve), but also the $\tilde{\pi}_1 + \tilde{\pi}_2$ combination (dot-dashed curve) gives a substantial contribution around invariant masses $M \approx$700–900 MeV/c^2.

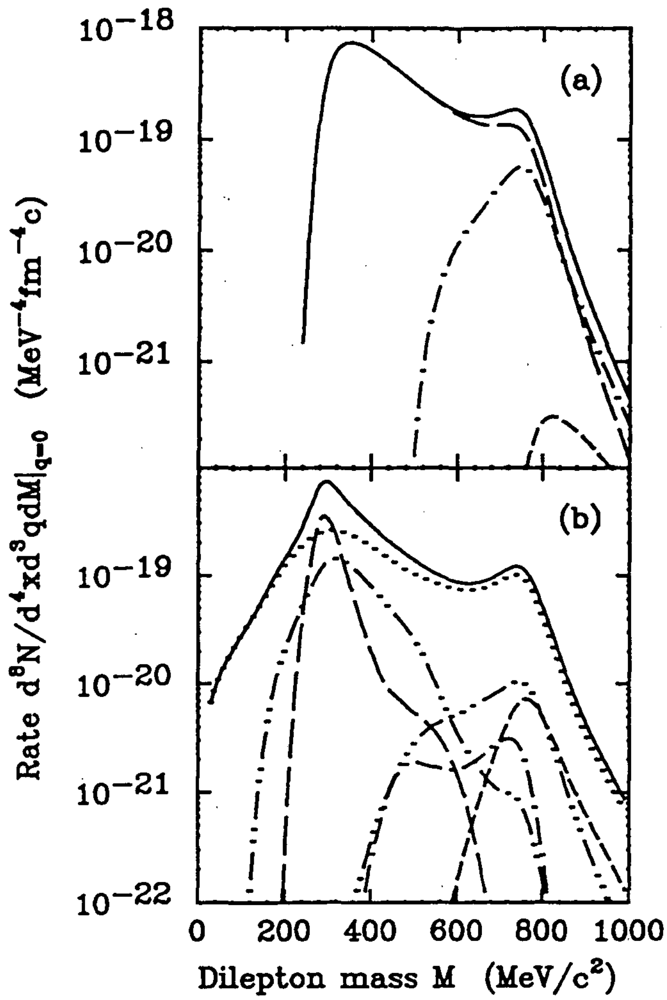

FIG. 3. Contribution to the total dilepton rate calculated at $\rho=\rho_0$ and T=100 MeV with the simple two-level model (a) and the more realistic model (b). The total rate (solid curve) is shown together with specific contributions from different combinations of spin-isospin modes: $\tilde{\pi}_1 + \tilde{\pi}_1$ (long-dashed), $\tilde{\pi}_1 + \tilde{\pi}_2$ (dot-dashed), $\tilde{\pi}_2 + \tilde{\pi}_2$ (short-dashed), $\tilde{\pi}_1 + j$ (dot-dot-dashed), $\tilde{\pi}_2 + j$ (dot-dot-dot-dashed), and $j + j$ (dotted), with j representing any mode other than $\tilde{\pi}_1$ or $\tilde{\pi}_2$.

In the $\pi + NN^{-1} + \Delta N^{-1}$ model (fig. 3b) there are many more combinations possible. To keep the figure somewhat readable we restrict ourselves to combinations of $\tilde{\pi}_1$, $\tilde{\pi}_2$ and j, where $j \neq \tilde{\pi}_1, \tilde{\pi}_2$. At low invariant mass, $M<250$ MeV/c^2, the main contribution comes from the combinations $j+j$ (dotted curve) and $j+\tilde{\pi}_1$ (dot-dot-dashed). As discussed above, it is the non-collective NN^{-1} modes that give the contribution to the j-modes at this low invariant mass region. In agreement with fig. 3a, the $\tilde{\pi}_1+\tilde{\pi}_1$ combination starts to contribute substantially around $M\approx280$ MeV/c^2. This contribution is also of similar magnitude as in fig. 3a. However, as seen in fig. 3b, the $\tilde{\pi}_1+\tilde{\pi}_1$ combination ceases to give a substantial contribution around $M\approx400$–600 MeV/c^2. This is because the mode $\tilde{\pi}_1$ enters the ΔN^{-1} continuum and gradually loses its collective character. The pionic strength is distributed among the non-collective ΔN^{-1} modes, which at the invariant masses $M\approx550$–800 MeV/c^2 give the main contribution to the j-modes (dotted curve). The dot-dot-dot-dashed curve represents the combination $\tilde{\pi}_2+j$. At lower invariant mass this is mainly $\tilde{\pi}_2+NN^{-1}$, while at larger masses it becomes mainly $\tilde{\pi}_2+\Delta N^{-1}$. Finally, the $\tilde{\pi}_1+\tilde{\pi}_2$ combination (dot-dashed curve) gives a similar contribution as in fig. 3a, but some of the strength of $\tilde{\pi}_1+\tilde{\pi}_2$ is taken over by the $\tilde{\pi}_2+\Delta N^{-1}$ combination (dot-dot-dot-dashed).

Nuclear collisions generate a range of densities and excitations and many different processes contribute to the dilepton yield. Transport simulations indicate that the dilepton yield at $M\approx200$–400 MeV/c^2 arises nearly exclusively from η and Δ Dalitz decay and pn bremsstrahlung [10]. However, since these processes occur in a medium and are correspondingly uncertain, it cannot be excluded that there is also some contribution from annihilation of NN^{-1} modes with a small pionic component. Whether such processes are in fact visible in actual heavy-ion collisions remains to be determined. This question is best addressed by means of dynamical simulations, but the implementation of these processes in the transport treatment is not a trivial task.

In summary, we have calculated the dilepton production arising from $\pi^+\pi^-$ annihilation in equilibrated nuclear matter. The results of a simple two-level ΔN^{-1} model used in previous works have been compared with the results of using a more realistic dispersion relation including π, NN^{-1}, and ΔN^{-1} excitations. We have found a substantial enhancement of the dilepton yield for invariant masses in the region $M<250$ MeV/c^2, arising from the annihilation of non-collective low-energy high-momentum NN^{-1} modes having a (very) small pion component. We have ignored the vertex corrections [5,6] which may reduce the dilepton yield somewhat. The evaluation of the dispersion relation at a temperature of T=100 MeV, rather than at zero temperature, does not affect the total dilepton yield much, but causes a significant degree of redistribution of the contributions from the different types of annihilation process.

Supported by the Swedish Natural Science Research Council, the National Institute for Nuclear Theory at the University of Washington in Seattle, and by the Director, Office of Energy Research, Office of High Energy and Nuclear Physics, Nuclear Physics Division of the U.S. Department of Energy (Contract DE-AC03-76SF00098).

[1] C. Gale and J.I. Kapusta, Phys. Rev. **C35**, 2107 (1987).
[2] C. Gale and J.I. Kapusta, Phys. Rev. **C38**, 2659 (1988).
[3] L.H. Xia, C.M. Ko, L. Xiong, and J.Q. Wu, Nucl. Phys. **A485**, 721 (1988).
[4] C.M. Ko, L.H. Xia and P.J. Siemens, Phys. Lett. **231B**, 16 (1989).
[5] C.L. Korpa and S. Pratt, Phys. Rev. Lett. **64**, 1502 (1990).
[6] C.L. Korpa, L. Xiong, C.M. Ko, and P.J. Siemens, Phys. Lett. **246B**, 333 (1990).
[7] L. Xiong, J.Q. Wu, Z.G. Wu, C.M. Ko, and J.H. Shi, Phys. Rev. **C41**, R1355 (1990).
[8] L. Xiong, Z.G. Wu, C.M. Ko, and J.Q. Wu, Nucl. Phys. **A512**, 722 (1990).
[9] Gy. Wolf, G. Batko, W. Cassing, U. Mosel, K. Niita, and M. Schäfer, Nucl. Phys. **A517**, 615 (1990).
[10] Gy. Wolf, W. Cassing, and U. Mosel, Nucl. Phys. **A552**, 549 (1993).
[11] J. Helgesson and J. Randrup, Preprint LBL-36359 (1994), Ann. Phys (in press).

LAWRENCE BERKELEY LABORATORY
UNIVERSITY OF CALIFORNIA
TECHNICAL AND ELECTRONIC
INFORMATION DEPARTMENT
BERKELEY, CALIFORNIA 94720